

# Tripartite Crosstalk between Cytokine IL-1 $\beta$ , NMDA-R and Misplaced Mitochondrial Anchor in Neuronal Dendrites Is a Novel Pathway for Neurodegeneration in Inflammatory Diseases

Dinesh C. Joshi,<sup>1\*</sup> Chuan-Li Zhang,<sup>1\*</sup> Deepali Mathur,<sup>1</sup> Alex Li,<sup>1</sup> Gaurav Kaushik,<sup>2</sup> Zu-Hang Sheng,<sup>3</sup> and Shing-Yan Chiu<sup>1</sup>

<sup>1</sup>Department of Neuroscience, School of Medicine and Public Health, University of Wisconsin–Madison, Madison, Wisconsin 53705, <sup>2</sup>Department of Orthopedics and Rehabilitation, University of Wisconsin–Madison, Madison, Wisconsin 53705, and <sup>3</sup>Synaptic Functions Section, Porter Neuroscience Research Center, National Institute of Neurological Disorders and Stroke, Bethesda, Maryland 20892

The mitochondrial anchor syntaphilin (SNPH) is a key mitochondrial protein normally expressed in axons to maintain neuronal health by positioning mitochondria along axons for metabolic needs. However, in 2019 we discovered a novel form of excitotoxicity that results when SNPH is misplaced into neuronal dendrites in disease models. A key unanswered question about this SNPH excitotoxicity is the pathologic molecules that trigger misplacement or intrusion of SNPH into dendrites. Here, we identified two different classes of pathologic molecules that interact to trigger dendritic SNPH intrusion. Using primary hippocampal neuronal cultures from mice of either sex, we demonstrated that the pro-inflammatory cytokine IL-1 $\beta$  interacts with NMDA to trigger SNPH intrusion into dendrites. First, IL-1 $\beta$  and NMDA each individually triggers dendritic SNPH intrusion. Second, IL-1 $\beta$  and NMDA do not act independently but interact. Thus, blocking NMDAR by the antagonist MK-801 blocks IL-1 $\beta$  from triggering dendritic SNPH intrusion. Further, decoupling the known interaction between IL-1 $\beta$  and NMDAR by tyrosine inhibitors prevents either IL-1 $\beta$  or NMDA from triggering dendritic SNPH intrusion. Third, neuronal toxicity caused by IL-1 $\beta$  or NMDA is strongly ameliorated in SNPH<sup>-/-</sup> neurons. Together, we hypothesize that the known bipartite IL-1 $\beta$ /NMDAR crosstalk converges to trigger misplacement of SNPH in dendrites as a final common pathway to cause neurodegeneration. Targeting dendritic SNPH in this novel tripartite IL-1 $\beta$ /NMDAR/SNPH interaction could be a strategic downstream locus for ameliorating neurotoxicity in inflammatory diseases.

**Key words:** dendrites; excitotoxicity; inflammation; mitochondria; multiple sclerosis; neurodegeneration

## Significance Statement

SNPH is a key mitochondrial protein normally expressed specifically in healthy axons to help position mitochondria along axons to match metabolic needs. In 2019 we discovered that misplacement of SNPH into neuronal dendrites causes a novel form of excitotoxicity in rodent models of multiple sclerosis. A key unanswered question about this new form of dendritic SNPH toxicity concerns pathologic molecules that trigger toxic misplacement of SNPH into dendrites. Here, we identified two major categories of pathologic molecules, the pro-inflammatory cytokines and NMDA, that interact and converge to trigger toxic misplacement of SNPH into dendrites. We propose that a dendritic mitochondrial anchor provides a novel, single common target for ameliorating diverse inflammatory and excitatory injuries in neurodegenerative diseases.

Received May 5, 2022; revised Aug. 1, 2022; accepted Aug. 7, 2022.

Author contributions: S.-Y.C., D.C.J., and C.-L.Z. designed research; D.C.J., C.-L.Z., and D.M. performed research; Z.-H.S. contributed unpublished reagents/analytic tools; S.-Y.C., D.C.J., C.-L.Z., D.M., A.L., and G.K. analyzed data; S.-Y.C. wrote the paper.

This work was supported by National Institute of Neurological Disorders and Stroke Grants R01 NS118198-01, R01 NS100924-01, and R21NS114844-01 to S.-Y.C. and the Intramural Research Program of the National Institute of Neurological Disorders and Stroke (Z.-H.S.). We thank Lance Rodenkirch (University of Wisconsin–Madison Optical Imaging Core) for fluorescence imaging support.

\*D.C.J. and C.-L.Z. share senior authorship.

The authors declare no competing financial interests.

Correspondence should be addressed to Shing-Yan Chiu at schiu1@wisc.edu.

<https://doi.org/10.1523/JNEUROSCI.0865-22.2022>

Copyright © 2022 the authors

## Introduction

In a normal neuron, the mitochondrial anchor syntaphilin (SNPH) is a key axon-specific mitochondrial protein that is crucial for neuronal health by positioning mitochondria along axonal microtubules to match local metabolic needs of axons (Kang et al., 2008). However, we recently discovered that in certain disease models, SNPH is misplaced into neuronal dendrites, causing excitotoxicity and dendritic pathology (Joshi et al., 2019). This novel excitotoxicity results from dendritic syntaphilin intrusion (DSI). Because dendrites are the summation point for synaptic

inputs that determine the net neuronal output, dendritic pathology resulting from misplacement of SNPH in dendrites (DSI) will have a major pathologic impact on neuronal performance in diseases.

This article addresses an important unanswered question regarding DSI, that is, what are the pathologic signals that trigger DSI? Diseases of the nervous system often involve interactions between different classes of pathologic molecules. The types of pathologic molecules determine the nature and scope of the disease. For example, if DSI is triggered by only one specific class of pathologic molecules, the relevance of DSI is narrowed to one type of disease. Alternatively, if different classes of pathologic molecules converge onto DSI, the disease scope of DSI will be significantly broadened. In this article, we initiated this investigation on the disease scope of DSI by exploring whether multiple classes of pathologic molecules interact to trigger DSI. We started with two different classes of pathologic molecules, the cytokine IL-1 $\beta$  and NMDA and examined if they interact to trigger DSI. Before the discovery of the neurotoxic DSI pathway (Joshi et al., 2019), the pro-inflammatory cytokine IL-1 $\beta$  and the glutamate receptor subtype NMDAR have been shown previously to interact in a reciprocal fashion to produce excitotoxicity (Viviani et al., 2003). The novel question is whether this IL-1 $\beta$ /NMDAR interaction converges onto DSI as a common downstream locus to cause neurotoxicity. If true, the disease scope of DSI would be significantly widened, making DSI a strategic common target to block diverse excitotoxic insults. Our results suggest a novel tripartite interaction among IL-1 $\beta$ , NMDAR, and dendritic SNPH underlying neurodegeneration in inflammatory diseases.

## Materials and Methods

Mice of either sex were used in this study. All experiments involving animals were performed in accordance with University of Wisconsin–Madison Research Animal Resources and Compliance. All animal usage and protocols were reviewed by the Animal Care and Usage Committee and approved by University of Wisconsin–Madison Research Animal Resources Center. Homozygous C57BL/6 SNPH<sup>-/-</sup> (SNPH-KO) mice were obtained from the Sheng laboratory at the National Institute of Neurological Disorders and Stroke.

**Primary cultures of hippocampal neurons.** Mouse primary hippocampal neurons were isolated from newborn postnatal day 0 (P0) C57BL6 WT and SNPH-KO (obtained from the Sheng laboratory at the National Institute of Neurological Disorders and Stroke). Briefly, P0 mice were decapitated, and hippocampi were isolated in ice-cold high glucose DMEM (HGD MEM) plus 10% fetal bovine serum (FBS). The hippocampi were rinsed twice with ice-cold HGD MEM and incubated with Papain (2 mg/ml prepared in HGD MEM) for 30 min at 5% CO<sub>2</sub> at 37°C. After digestion in papain, DNase was added (2.5 mg/ml prepared in HGD MEM) for 30 s followed by the addition of 10% FBS to inactivate DNase. The digested tissue was gently triturated by pipetting and filtered through a 100  $\mu$ m sterile cell strainer and spun at 800 rpm for 10 min at room temperature (RT). Cell pellets were resuspended in a 3:1 ratio of neurobasal-B27 and HGD MEM (with 10% fetal bovine serum) and plated on poly-D-lysine-coated (0.2 mg/ml) coverslips at a density of 1.1  $\times$  10<sup>5</sup> cells/ml. The plated neurons were switched to neurobasal B27 medium after 5 h and were treated with 1  $\mu$ M Ara-C after 48 h of plating for 48 h to inhibit the growth of non-neuronal cells in the culture. Cells were then maintained in neurobasal B27 medium with one-third of the media changed every 48 h. DSI experiments were performed on neurons cultured for 9–12 d.

**Organotypic slice cultures from mice.** Organotypic slice cultures were prepared according to Rakotomamonjy and Guemez-Gamboa (2019), with modifications. Before dissection, we autoclaved surgical tools and disinfected all surface areas and items to be used with 70% ethanol. A six-well culture plate was filled with culture medium [serum-containing

medium (SCM)] containing 50% MEM with Earle's salts, 25% heat-inactivated horse serum, 25% Earle's balanced salt solution supplemented with glutamax (1 mM), penicillin/streptomycin (100 unit/ml), glucose (6.5 mg/ml), and fungizone (2  $\mu$ g/ml). Each well was filled with 1 ml of culture medium and preincubated at 37° for at least 1 h. P8–P11 C57BL6 WT mice were used for culturing cerebellar organotypic slices. The mice were decapitated quickly using straight operating scissors. The whole brain was taken out and transferred to a 60 mm dish filled with cold HBSS plus 5 mg/ml glucose. The cerebellum was dissected from the brain and isolated from the brainstem by cutting through the cerebellar peduncles. The cerebellum was placed on the plate of a McIlwain Tissue Chopper (Ted Pella), and 350  $\mu$ m thick sagittal slices were cut with the chopper. The cerebellar slices were separated from each other using a microprobe. Good-quality sections were taken out with plastic transfer pipettes and placed in the culture inserts in a six-well plate with preincubated culture medium. Three to four cerebellum slices were transferred in each insert, and the six-well culture plate was transferred to the incubator at 37° and 5% CO<sub>2</sub>. This was referred to as day 0. The medium was completely changed every 2 d. On day 2, the culture medium was replaced with 1 ml of SCM. On day 4, the medium was replaced with two-thirds SCM plus serum-free medium (SFM) containing DMEM and Nutrient Mixture F-12 with glutamax (1 mM), 1% B27, 0.5% N<sub>2</sub>, penicillin/streptomycin (100 unit/ml), and fungizone (2  $\mu$ g/ml). On day 6, the medium was changed to one-third SCM plus two-thirds SFM. On day 8 and later, we only applied SFM until slices are fixed and stained with SNPH (to monitor possible DSI) and Calbindin (to label Purkinje cells and dendrites).

**Immunofluorescence and image acquisition.** For antibody labeling in primary neurons, we fixed coverslips containing neuronal cells with 4% paraformaldehyde (PFA) and 4% sucrose (Kang et al., 2008) in PBS for 20 min at RT followed by permeabilization with 0.3% Triton X-100 for 15 min and blocking in 10% serum for 1 h at RT. The neurons were then incubated with primary antibody MAP-2 (1:500; Millipore), SNPH (1:500; catalog #ab192605, Abcam) and PSD95 (1:200; NeuroMab) antibodies overnight at 4°C. The following day these coverslips were washed three times (5 min each) with PBS and incubated with fluorescently conjugated Alexa Fluor secondary antibodies and mounted on glass slides using UltraCruz Aqueous Mounting Medium. Fluorescent images were acquired using a Nikon A1 confocal microscope with 60 $\times$  (1.4 numerical aperture) plan apochromatic oil-immersion objectives at 1024  $\times$  1024 resolution. The optical thickness was set at 0.25  $\mu$ m and 3-D volume scans (*z*-series) images were collected from randomly selected fields. Optical settings were kept identical for all the experimental groups to ensure comparability between experimental groups. Image analysis was accomplished using Nikon Elements, ImageJ (National Institutes of Health), Huygens (Scientific Volume Imaging), and Imaris (Bitplane) software.

**Viral transduction of mito-mCherry.** Cultures of mouse primary hippocampal neurons were transduced with mito-mCherry to pretag mitochondria. Briefly, adeno-associated virus mito-mCherry viral particles were added to neuronal cultures on days 4–5 *in vitro* for 72–96 h, and cultures were washed three times with 1 $\times$  PBS and fixed with 4% paraformaldehyde for 20 min at ambient temperature. Cultures were washed three times with 1 $\times$  PBS and processed for SNPH and MAP2 antibody labeling.

**Orthogonal analysis of dendritic SNPH (DSI).** Dendritic SNPH is measured by orthogonal analysis. Cultured neurons were stained with MAP2 to identify dendrites and SNPH to identify DSI. To verify that SNPH is inside dendrites, orthogonal images at three different angles were obtained using NIS-Elements software (Nikon) with a 60 $\times$  oil lens under a Nikon A1RS Confocal Microscope at the University of Wisconsin–Madison Optical Imaging Core to confirm that SNPH immunoreactivity originates from inside the MAP2-positive dendrites. To quantify DSI, we first open the 3D images with NIS-Elements to identify if yellow puncta (SNPH) are inside red dendrites (green puncta, SNPH, are outside dendrites) by orthogonal analysis under 1000 $\times$  magnification. At the same time, we open the same image with ImageJ software on another computer to draw contours of all SNPH immunoreactivity (yellow puncta) within the total MAP2 area (red

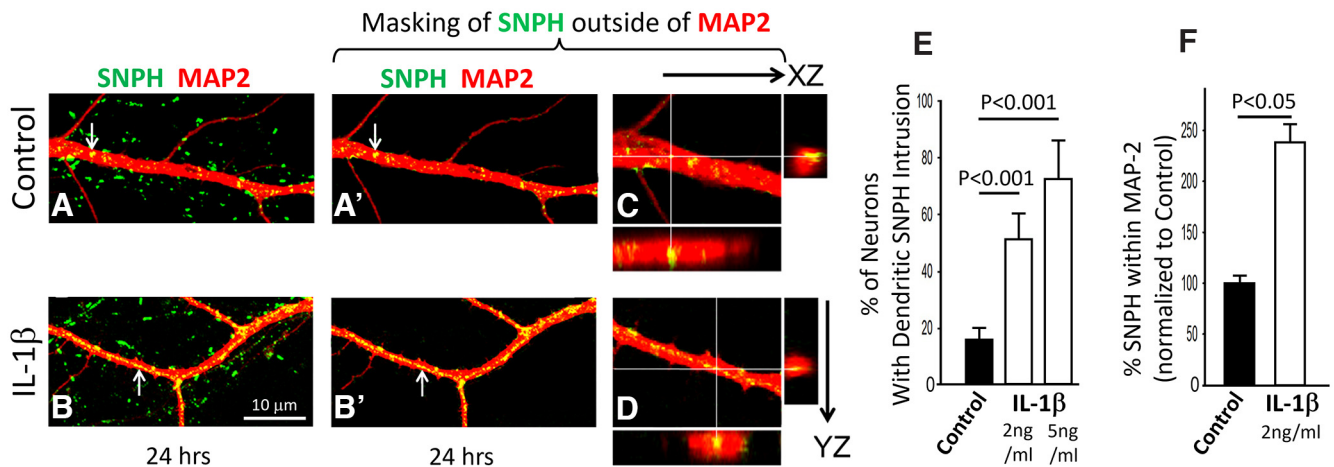


**Figure 1.** IL-1 $\beta$  triggers DSI; orthogonal analysis. Cultured hippocampal neurons were stressed with IL-1 $\beta$  for 24 h then double stained with SNPH and MAP2 (dendrites) for DSI assays. **A**, Control; SNPH puncta were present in axons (MAP2-negative) but rarely in dendrites (MAP2-positive). **B**, IL-1 $\beta$ ; lines of SNPH puncta were superimposed (arrow, yellow) on the MAP2-positive dendrites. Scale bar, 10  $\mu$ m. **A'**, **B'**, **C**, **D**, Masking was used to eliminate the MAP2-negative SNPH puncta outside the dendrites, and orthogonal analysis was conducted to see if the yellow SNPH puncta were outside or inside the dendrites (**C**, **D**). In the control (**C**), the yellow SNPH puncta were lying on the surface (presumably from unlabeled axons) impinging into the dendrites as shown by the green that transitions into yellow. In contrast, in IL-1 $\beta$  (**D**) the yellow SNPH puncta are exclusively inside the dendrite (i.e., DSI). **E**, Percentage of neurons with DSI increased by IL-1 $\beta$  ( $N = 15$  neurons in 3 experiments). **F**, Orthogonal analysis shows IL-1 $\beta$  triggers significant increase in percentage of SNPH within MAP-2 area ( $N = 8$  dendrites in 3 experiments; Extended Data Figure 1-1).

areas) within the fixed frame. This fixed frame is standardized and applied to all samples. Both areas of yellow and red are measured and recorded by ImageJ and saved in Microsoft Excel. Finally, DSI is computed as the total SNPH area divided by the total MAP2 area for a particular dendritic segment under analysis with Excel. Analysis was performed by one of us who was blinded to the experimental conditions.

**Neuronal viability.** Neuronal survival in IL-1 $\beta$  or NMDA stress experiments was quantitated using morphologic criteria. Neurons from SNPH<sup>+/+</sup> and SNPH<sup>-/-</sup> mice grown on coverslips were treated with NMDA or IL-1 $\beta$  for 30 min in growth medium, washed three times with growth media, placed back in a CO<sub>2</sub> incubator, and neuronal viability was determined after 24 h (Wang and Schwarz, 2009; Joshi et al., 2011). A neuron with good neuritic arborization and distinct cell soma was considered healthy, whereas a neuron with fragmented neurites and cell soma was considered dead (Joshi et al., 2011). We also confirmed this morphologic criterion with a propidium iodide (PI) assay, which only stains dead cells (Ying et al., 2001; Jiajia et al., 2017).

**Statistical analysis.** Data are presented as the mean  $\pm$  SEM. Statistical differences in measured variables between the experimental and control groups were assessed by Student's *t* test, and  $p < 0.05$  was considered statistically significant.

## Results

The goal of this study is to identify pathologic molecules that trigger misplacement or intrusion of SNPH in dendrites (DSI). We focused on two well-established excitotoxicity pathways (IL-1 $\beta$  and NMDA) and examined whether they trigger DSI in an interactive fashion to exacerbate neurotoxicity. Using primary cultures of hippocampal neurons, we first examined if IL-1 $\beta$  and NMDA individually trigger DSI before addressing if they interact.

### IL-1 $\beta$ triggers DSI in cultured hippocampal neurons

SNPH is normally specific for axons and is absent or expressed in very low density in the dendrites. Here, we examined if stressing cultured neurons with IL-1 $\beta$  triggers a selective increase or intrusion of SNPH into dendrites (DSI). Because dendrites are sometimes intertwined with axons in culture because of synapse formation, care must be exercised to distinguish SNPH that has

invaded inside dendrites from SNPH normally present in axons but in close proximity outside dendrites. We used two independent methods to examine if IL-1 $\beta$  triggers DSI in cultured hippocampal neurons.

#### Method 1

Neurons were stressed with IL-1 $\beta$  for 24 h then fixed and stained for MAP2 (dendrites and soma) and SNPH (Fig. 1A,B). Interestingly, masking of SNPH outside MAP2 dendrites (Fig. 1A',B') shows a clear picture of a string of SNPH (yellow, arrow) within dendrites stressed by IL-1 $\beta$  (Fig. 1B') but not control (Fig. 1A'). Using orthogonal analysis, we determined that the SNPH yellow puncta in the IL-1 $\beta$  stressed dendrite are inside the dendrite (Fig. 1D). In contrast, the SNPH puncta in the control (Fig. 1C) are outside and on the surface of the dendrite as revealed by the green signal that impinges on the dendrite and turns yellow. The SNPH puncta outside dendrites in (Fig. 1C) are presumably from overlying axons making synaptic contacts with dendrites in culture. Stress with IL-1 $\beta$  markedly increases the percentage of neurons with DSI (Fig. 1E). Correspondingly, DSI, measured as the percentage of the SNPH area inside the dendritic area (i.e., within the MAP-2 area) in orthogonal analysis (Fig. 1C,D), undergoes a significant increase (Fig. 1F).

#### Method 2

Because induction of DSI by a pathologic signal is an important new finding that is key to this article, we next used an independent method to confirm DSI induction by IL-1 $\beta$ . In this method, we used viral transduction to pretag mitochondria with mito-mCherry, then used the pretagged mitochondria inside dendrites to identify SNPH that has invaded inside dendrites and binds to the pretagged mitochondria by 3-D rotation. The neuronal cultures were double labeled with SNPH and the dendritic marker MAP2. We first used MAP2 to identify a dendritic segment, then focused on possible DSI in the dendritic segment by examining the colabeling of SNPH with the pretagged mito-mCherry. In the following data presentation, only SNPH and mito-mCherry signals on the dendrite are shown. Figure 2A shows 3-D rotation of a control dendrite and a IL-1 $\beta$  stressed dendrite. As an example,



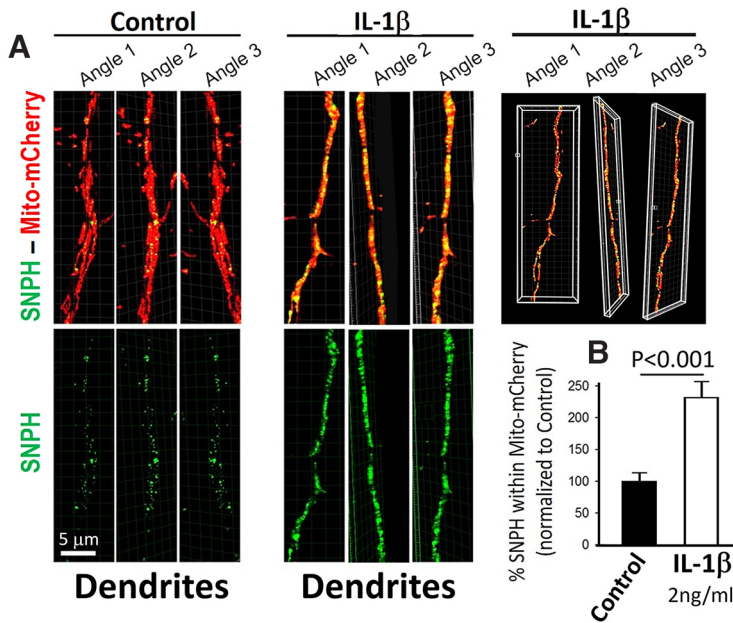


**Figure 2.** IL-1 $\beta$  triggers DSI; viral transduction with mito-mCherry. **A**, Viral transduction of mito-mCherry was used to pretag dendritic mitochondria to capture SNPH intrusion inside dendrites by corotation. Dendrites were identified by MAP-2 staining (data not shown). SNPH inside dendrites will turn yellow when it binds to red mito-mCherry and will remain yellow during corotation, shown on the far right for IL-1 $\beta$  (2 ng/ml, 24 h) stressed dendrites. Scale bar, 5  $\mu$ m. **B**, Quantification of percentage of SNPH within mito-mCherry in Control and IL-1 $\beta$  ( $N = 8$  dendrites in 3 experiments).

the actual rotation angles are shown on the far right for the IL-1 $\beta$  dendrite. The pretagged mitochondria inside dendrites are red. Any intrusion of SNPH into dendrites would turn yellow when SNPH binds to the mitochondria. Importantly, we further used 3-D rotation to show that the yellow signal remains Yellow at three different angles of rotation confirms that the SNPH signal comes from within the dendrite. Extensive DSI (yellow puncta; Fig. 2A, top) are seen in dendrite stressed by IL-1 $\beta$  compared with control. The percentage of SNPH within mito-mCherry shows a significant increase in IL-1 $\beta$  (Fig. 2B). Importantly, these two independent methods yield similar increase of SNPH in dendrites when stressed by IL-1 $\beta$  (compare Figs. 1F, 2B). Collectively, these two independent methods (Figs. 1, 2) led to the first identification of an important pathologic signal that triggers DSI, the pro-inflammatory cytokine IL-1 $\beta$ .

#### Specificity of IL-1 $\beta$ on DSI

Although Figures 1 and 2 demonstrated that DSI is triggered by IL-1 $\beta$ , an important issue is whether the IL-1 $\beta$ /DSI crosstalk is a highly spatially specific pathologic phenomenon or merely reflects nonspecific alterations of protein expression/distribution in unhealthy neurons under inflammation stress. We addressed this issue (Extended Data Figure 1-1) by examining dendritic specificities of the IL-1 $\beta$ /DSI crosstalk in primary neuronal cultures. Extended Data Figure 1-1 shows that IL-1 $\beta$  selectively triggers an abnormal increase of SNPH in dendrites (DSI) without affecting expression of another dendritic protein, the spine-specific PSD-95. In addition to primary cultures, we also confirmed the spatial specificity of IL-1 $\beta$ /DSI crosstalk in preparations with intact neuronal connectivity using organotypic brain slices (Fig. 3). We started with neonatal cerebellar organotypic slices and added IL-1 $\beta$  (2 ng/ml) after 7 d in culture as shown in Figure 3. Slices were double stained with SNPH (Fig. 3A,B) to

monitor possible DSI and Calbindin to label dendrites of Purkinje cells (PC; Fig. 3C,D). Corresponding merged SNPH-Calbindin images are shown in Figure 3, E and F. Control without IL-1 $\beta$  shows virtually no SNPH in the dendritic layers (Fig. 3A,C,E). In contrast, IL-1 $\beta$  triggers massive and selective SNPH expression in the dendritic regions of PC (Fig. 3B,D,F). Orthogonal analysis of high-magnification regions showed that SNPH triggered by IL-1 $\beta$  is located inside dendrites (Fig. 3Hj). Hence, IL-1 $\beta$  triggers the selective increase of SNPH in dendrites (DSI) in organotypic slices. Apparently, IL-1 $\beta$  also triggers massive synthesis of SNPH as evidenced by the increase in SNPH in the PC soma regions (Fig. 3B), but this increased SNPH synthesis is selectively misplaced into the dendrites (Fig. 3B,F). Figure 3 shows that in a complex neuron-glia network, the action of IL-1 $\beta$  on SNPH is highly selective at neuronal dendrites, confirming primary culture data that IL-1 $\beta$  selectively triggers DSI.

Collectively, Figure 3 and Extended Data Figure 1-1 show that the pathology of IL-1 $\beta$ /DSI crosstalk is highly dendritic specific and not a generalized, nonspecific damaging phenomenon. Having confirmed the specificity of IL-1 $\beta$ /DSI crosstalk in both primary cultures and organotypic slices, for the rest of this article we use primary cultures to characterize DSI where experimental parameters can be much better controlled.

#### SNPH-KO protects against IL-1 $\beta$ toxicity

As IL-1 $\beta$  triggers DSI, and DSI has been shown in our previous study to be toxic to neurons (Joshi et al., 2019), the logical next step is to see if IL-1 $\beta$  causes toxicity and whether this toxicity is protected by SNPH-KO. In Figure 4 we therefore applied IL-1 $\beta$  stress (2, 2.5, 5, 10 ng/ml) to wild-type SNPH ( $^{+/+}$ ) neurons and SNPH ( $^{-/-}$ ) neurons cultured from SNPH-KO mice. After 24 and 72 h, neurons were stained with the dendritic marker MAP2 for toxicity analysis by measuring neuronal loss (Fig. 4, left) and dendritic loss (Fig. 4, right).

#### Neuronal death assays

For neuronal death assays (Fig. 4, left, Morphology), we used morphologic criteria and counted MAP2-positive neuronal soma density under IL-1 $\beta$  stress normalized to control without IL-1 $\beta$ . SNPH $^{+/+}$  and SNPH $^{-/-}$  neurons were plated at equal density before IL-1 $\beta$  treatment. After IL-1 $\beta$  treatment, significant loss of MAP2-positive neurons was seen in the SNPH $^{+/+}$  group. In contrast, in the SNPH $^{-/-}$  group, loss of MAP2-positive neurons under IL-1 $\beta$  stress was completely prevented at 24 h at 2.5, 5, and 10 ng/ml and was significantly prevented at 72 h at 10 ng/ml (Fig. 4, left, Morphology, bar charts). We also corroborated morphologic assay of neuronal death with PI staining (Fig. 4, left, PI staining). PI is a red fluorescent viability dye that is excluded from live cells but penetrates and binds to DNA in dead or compromised cells. The images in the PI staining box show live staining of (PI)/Calcein in cultured neurons to examine if IL-1 $\beta$  toxicity is protected by SNPH-KO. PI uptake labels dead cells, whereas Calcein uptake labels live cells. Images show live PI/Calcein staining in SNPH $^{+/+}$  and SNPH $^{-/-}$  neurons before and after IL-1 $\beta$  stress (Fig. 4A–D; 2 ng/ml, 24 h). Other

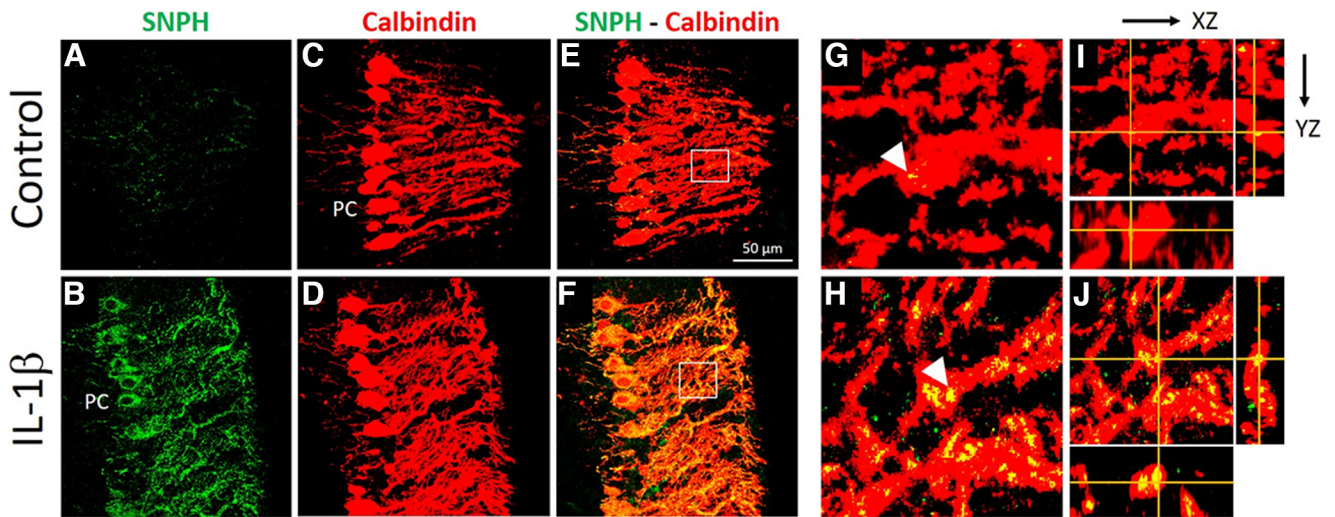


**Figure 3.** Specificity of DSI in cerebellar organotypic slice under IL-1 $\beta$  stress. Cerebellar organotypic slices from P11 mice were cultured for 7 d before treatment with 2 ng/ml IL-1 $\beta$  for 24 h before fixation for analysis. **A, B**, SNPH staining in control and IL-1 $\beta$ -treated slice. Note massive SNPH increase in dendritic layer of PC. **C, D**, Calbindin staining of PC dendrites. **E, F**, Merged SNPH-Calbindin shows IL-1 $\beta$  triggers massive SNPH in dendritic layers (orange). **G, H**, SNPH is inside dendrites (DSI) in high magnification (arrowhead) shown by orthogonal analysis (**I, J**).

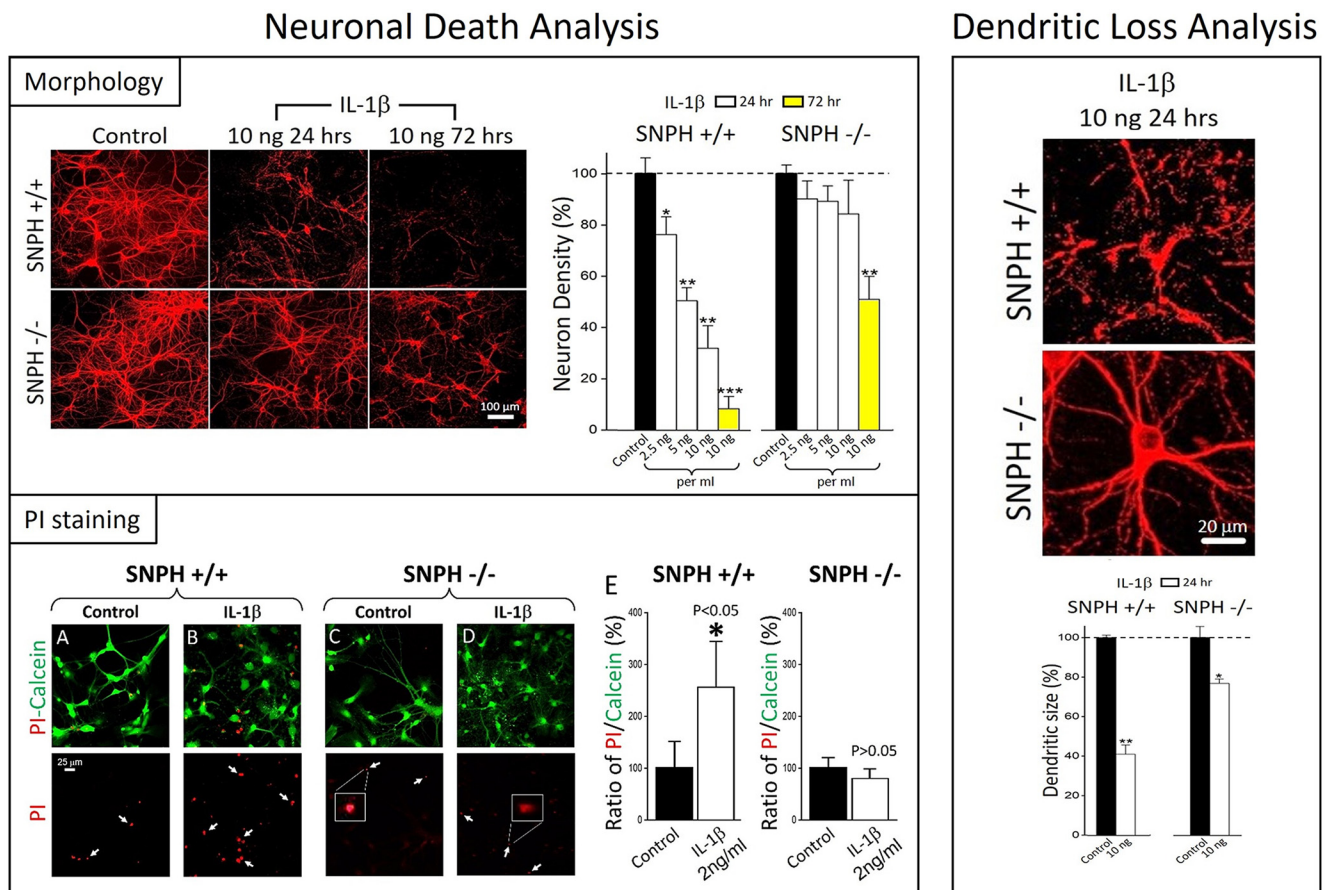


**Figure 4.** IL-1 $\beta$  neurotoxicity protection by SNPH-KO. Neuronal death analysis (left) and dendritic loss analysis (right) for primary cultures of hippocampal neurons. Top left, Morphology. Cultures were plated at equal density and stained with MAP2. Neuronal death was assayed by counting MAP2-positive neuronal soma density. Left, Representative images of cultured hippocampal SNPH<sup>+/+</sup> and SNPH<sup>-/-</sup> neurons under IL-1 $\beta$  stress (10 ng/ml) for 24 and 72 h. Right, Quantitative analysis of MAP2-positive neuron density. Bottom, PI staining. **A–D**, Cultured primary hippocampal SNPH<sup>+/+</sup> (**A, B**) and SNPH<sup>-/-</sup> (**C, D**) neurons were treated with IL-1 $\beta$  (2 ng/ml, 24 h) then stained with live PI/Calcein LIVE/DEAD Cell Imaging Kit (catalog #488/570, Invitrogen) for 15 min. Bottom, Corresponding PI images alone. White arrows show examples of red PI puncta. **E**, Quantification of PI/Calcein ratio by counting PI puncta and Calcein-positive cell bodies with ImageJ software. IL-1 $\beta$  increases the proportion of dead cells in SNPH<sup>+/+</sup> but not in SNPH<sup>-/-</sup> neurons.  $N = 3$  Petri dishes each group, and 10 images per dish collected for analysis. Top right, Dendritic loss analysis. Top, High-magnification images of SNPH<sup>+/+</sup> and SNPH<sup>-/-</sup> neurons 24 h after 10 ng IL-1 $\beta$ . Bottom, Normalized counts of dendrites (>30  $\mu$ m length) per neuron relative to control (no IL-1 $\beta$ ). All graphs represent the mean  $\pm$  SEM; \* $p < 0.05$ , \*\* $p < 0.01$ ; \*\*\* $p < 0.005$  ( $N = 3$  Petri dishes in each group).



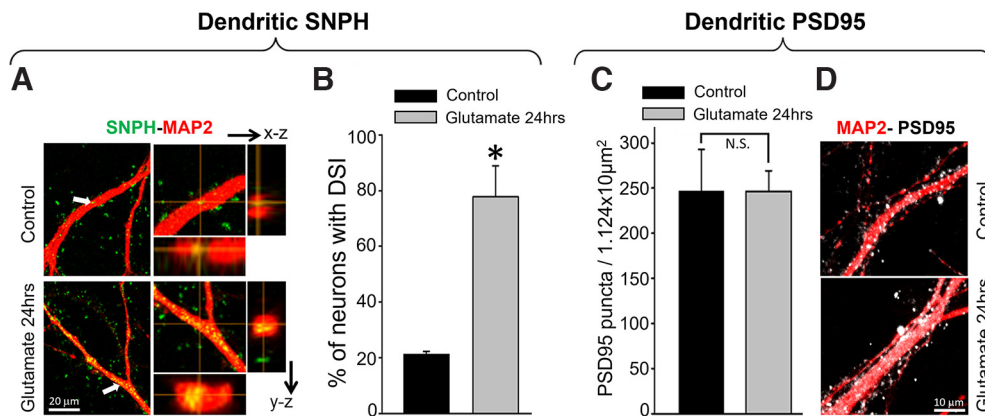


**Figure 5.** Elevation of extracellular glutamate causes dendritic SNPH intrusion in cultured neurons. **A**, Hippocampal neurons treated with 5  $\mu\text{M}$  (Glutamate) or 0  $\mu\text{M}$  (Control) in culture medium for 24 h and stained for SNPH, MAP2, and PSD95 (postsynaptic marker). Left, Colocalization (yellow) of SNPH and MAP2 shows SNPH within dendrites in Glutamate-treated neurons. Right, Orthogonal slice view of yellow puncta (left, arrows) confirming SNPH punctum within dendrites (yellow in both x-z and y-z orientation) of Glutamate-treated neuron, whereas SNPH punctum in control shows they impinged from the outside surface (green and yellow in x-z and y-z orientation). **B**, Quantification of neurons with SNPH intrusion in Control ( $n = 18$  neurons) and Glutamate ( $n = 24$  neurons)-treated cultures ( $*p < 0.05$ ). **C**, Quantification of PSD95 puncta in Control ( $n = 5$  dendrites) and Glutamate ( $n = 5$  dendrites)-treated neurons showing no change in PSD95 expression. **D**, Representative images of MAP2 (red)-PSD95 (pseudo colored as gray) expression in Control and Glutamate-treated neurons from **A**.

images show corresponding PI stain alone. IL-1 $\beta$  triggers significant increase in PI puncta in SNPH<sup>+/+</sup> (Fig. 4B, bottom) but not in SNPH<sup>-/-</sup> neurons (Fig. 4D, bottom). Quantification of PI/Calcein ratio (Fig. 4E) shows the proportion of dead cells increased in SNPH<sup>+/+</sup> neurons under IL-1 $\beta$  stress but were completely protected in SNPH<sup>-/-</sup> neurons. Collectively, two independent assays of toxicity (counting MAP2-positive neuron density and assaying PI uptake) demonstrated that IL-1 $\beta$  toxicity in neuronal culture is protected by SNPH-KO.

#### Dendritic loss assays

Stress by IL-1 $\beta$  not only causes neuronal death but also fragmentation of dendritic arbors. For dendritic fragmentation assays (Fig. 4, right), dendritic size in surviving neurons in IL-1 $\beta$  (10 ng/ml 24 h) was assayed by counting the number of intact dendrites (>30  $\mu\text{m}$ ) per neuron then normalized to control (Fig. 4, bar chart at bottom). High-magnification images show (Fig. 4, top) IL-1 $\beta$  induces extensive dendritic fragmentation in SNPH<sup>+/+</sup> but not in SNPH<sup>-/-</sup>. How might SNPH-KO protect against IL-1 $\beta$  toxicity? We hypothesize that SNPH-KO abolishes the toxic DSI triggered by IL-1 $\beta$ , thereby preventing dendritic damage and ultimate neuronal death.

#### Glutamate triggers DSI in cultured hippocampal neurons

Having established IL-1 $\beta$  as a pathologic signal that triggers DSI, we next examined another possible pathologic signal for DSI that might interact with IL-1 $\beta$ , namely, glutamate. It is well known that IL-1 $\beta$  is linked to excitotoxicity. Likewise, excessive glutamate is also a pathologic signal for excitotoxicity. The resting *in vivo* [Glu]<sub>ext</sub> is estimated to be in the nM range both in synaptic and nonsynaptic regions (Chiu and Jahr, 2017) and could rise to several hundred  $\mu\text{M}$  during synaptic activity in pathologic conditions, particularly when the glutamate transporter is blocked (Jaubaudon et al., 1999; Danbolt, 2001; Herman and Jahr, 2007). We therefore selected a sublethal dosage of 5  $\mu\text{M}$  to examine possible induction of DSI by glutamate without the confounding factor of massive cell death. Figure 5A shows that treating cultured hippocampal neurons with 5  $\mu\text{M}$  glutamate for 24 h triggered DSI by orthogonal analysis. The number of neurons with DSI is dramatically increased in glutamate (Fig. 5B). Similar to IL-1 $\beta$ , glutamate triggers DSI but does not cause

nonspecific upregulation of dendritic proteins. Thus, glutamate selectively recruits SNPH to the dendrites (Fig. 5A,B) without altering the spatial expression pattern of the spine specific PSD95 (Fig. 5C,D). Further, dendritic SNPH intrusion triggered by glutamate is not a consequence of cell death, as the sublethal glutamate treatment prevented massive cell death. Although higher glutamate concentrations at longer treatment times will kill cells, our sublethal glutamate treatment at 24 h apparently unmasks an early event of dendritic SNPH intrusion triggered by glutamate itself.

#### NMDAR is a glutamate receptor subtype that triggers DSI

Having demonstrated that glutamate triggers DSI, we next asked in Figure 6 which glutamate receptor subtypes are responsible for triggering DSI. We used MK-801 to block the ionotropic NMDAR subtype and LY-36738 to block the metabotropic glutamate subtype (mGluR). Figure 6 shows that the DSI induced by glutamate (24 h; Fig. 6B) over control (Fig. 6A) was blocked by MK-801 (Fig. 6C). Orthogonal analysis of respective images are shown (Fig. 6D,E,F) to confirm DSI. The average results for MK-801 are shown in Figure 6G, demonstrating that MK-801 completely blocks glutamate from inducing DSI. In contrast, LY-36738 does not block the DSI induced by glutamate ( $p > 0.05$ ). We therefore suggest that NMDAR is a key receptor subtype underlying DSI induction by glutamate. To further corroborate this result, we directly treated cultured neurons with NMDA. Figure 6 shows that a 24 h treatment with 10  $\mu\text{M}$  NMDA induces DSI (Fig. 6I) over control (Fig. 6H) that is blocked by MK-801 (Fig. 6J) with corresponding orthogonal images verifying DSI (Fig. 6K–M). Extended Data Figure 6-1 validates the specificity of the SNPH antibody used to detect SNPH by showing that the SNPH immunoreactivity detected by the SNPH antibody during NMDA treatment completely disappears in SNPH-KO cultures. Average results for DSI induction by NMDA and blockage by MK-801 are shown in Figure 6N. Collectively, we have established that glutamate is a signaling molecule that triggers DSI and that a major glutamate receptor subtype that triggers DSI is NMDAR.

#### SNPH-KO protects against NMDA toxicity

We demonstrated earlier that IL-1 $\beta$  triggers DSI and SNPH-KO ameliorates IL-1 $\beta$  toxicity (Fig. 4). Having now demonstrated

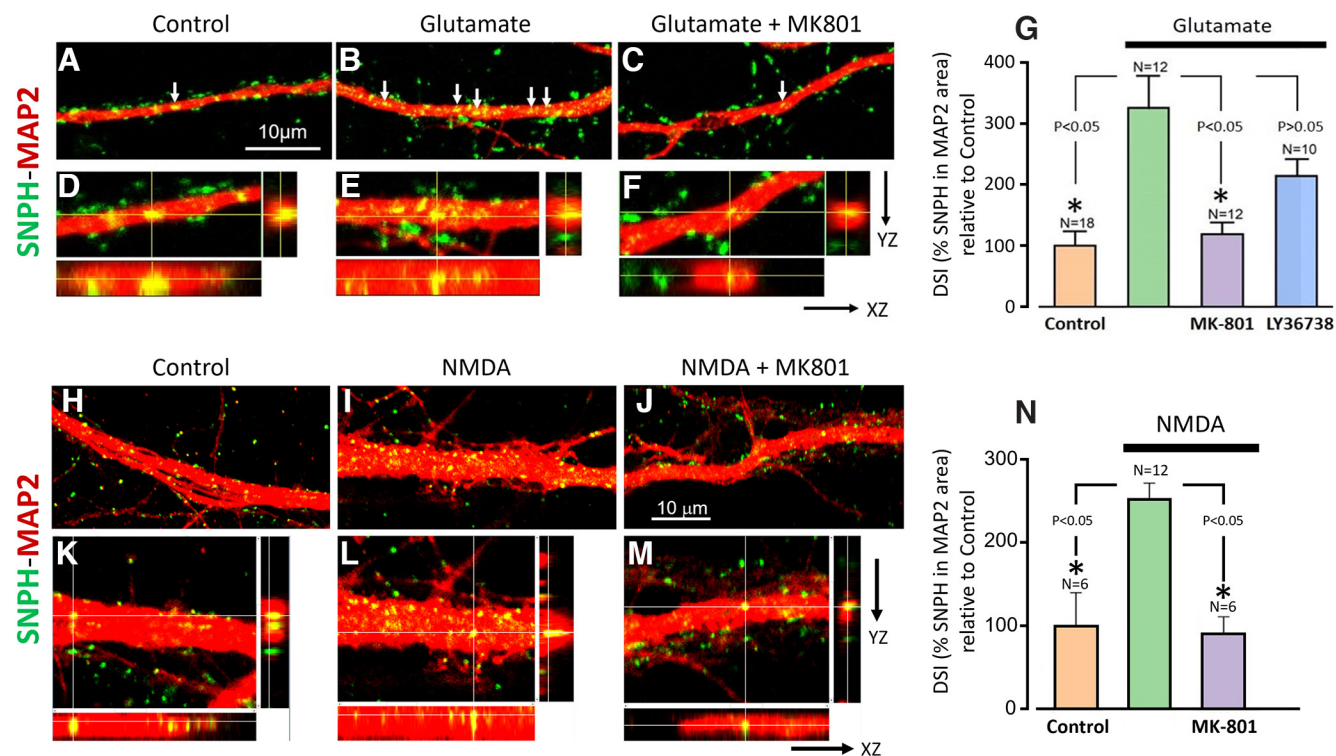


**Figure 6.** NMDAR is a glutamate receptor subtype that triggers DSI. Top, Primary cultures of hippocampal neurons were treated with Glutamate ( $5 \mu\text{M}$ ) in the presence or absence of MK-801 ( $5 \mu\text{M}$ ) and LY36738 ( $50 \mu\text{M}$ ) for 24 h and labeled for SNPH and MAP2 antibodies to identify DSI. MK-801 blocks NMDAR, and LY36738 blocks mGluR. **A–C**, Representative images of Control, Glutamate, and Glutamate + MK801. White arrows show yellow puncta of possible SNPH (green) intrusion into dendrites (red). **D–F**, Orthogonal slice view of yellow puncta confirming SNPH punctum inside dendrites (yellow in both x-z and y-z orientation) in these groups. **G**, Quantitative analysis of SNPH area within the dendritic MAP2 area from indicated numbers (N) of dendrites shown. Note that MK-801 completely inhibits dendritic SNPH intrusion triggered by glutamate ( $p < 0.05$ \*,  $N = 12$ ). In contrast, LY36738 fails to block SNPH intrusion triggered by glutamate ( $p > 0.05$ ,  $N = 10$ ). Hence, NMDAR mediates dendritic SNPH intrusion. Bottom, Primary cultures of hippocampal neurons were treated with NMDA ( $10 \mu\text{M}$ , 24 h) in the presence or absence of MK-801 ( $5 \mu\text{M}$ ). **H–J**, NMDA induces DSI (yellow puncta, **I**) over Control (**H**) that is blocked by MK801 (**J**). **K–M**, Orthogonal slice view of yellow puncta confirms SNPH is inside dendrites. **N**, Quantitative analysis of NMDA results showing the DSI induced by NMDA ( $p < 0.05$ \*,  $N = 12$ ) is blocked by MK-801 ( $p < 0.05$ \*,  $N = 6$ ; Extended Data Figure 6-1).

that NMDA also triggers DSI, we next similarly asked if SNPH-KO also ameliorates NMDA toxicity. In our previous study (Joshi et al., 2019) we showed that a brief 30 min treatment of cultured hippocampal neurons with  $10 \mu\text{M}$  NMDA did not induce neuronal cell death at 24 h, unless the neurons were pre-transfected with SNPH plasmids to artificially reconstitute DSI before the 30 min NMDA treatment. It is possible that in our previous study (Joshi et al., 2019) the brief 30 min NMDA treatment did not trigger sufficient DSI to kill neurons. As we have now demonstrated that a prolonged 24 h treatment with  $10 \mu\text{M}$  NMDA induced DSI (Fig. 6N), a logical question is whether self-induction of DSI by NMDA over a 24 h treatment leads to toxicity. We therefore examined if a 24 h NMDA treatment produces loss of MAP2-positive neurons and whether this neuronal loss can be protected by SNPH-KO. Figure 7 shows that a 24 h treatment with 20, 50, and  $100 \mu\text{M}$  NMDA induces neuronal loss in SNPH<sup>+/+</sup> neurons and the degree of protection offered by SNPH<sup>-/-</sup> neurons. Stress by  $20 \mu\text{M}$  NMDA caused an ~50% loss of MAP2-positive neurons in SNPH<sup>+/+</sup> cultures that is completely protected in SNPH<sup>-/-</sup> cultures (Fig. 7B). Even at the highest concentration of  $100 \mu\text{M}$  NMDA, which caused a ~90% loss of MAP2-positive neurons in the SNPH<sup>+/+</sup> cultures (Fig. 7B, left), this loss is still significantly protected in the SNPH<sup>-/-</sup> cultures (Fig. 7B, right). Hence, we suggest that as in the case of IL-1 $\beta$ , the self-induction of DSI by NMDA during prolonged treatment contributes to NMDA toxicity and this toxicity can be ameliorated by SNPH-KO.

### IL-1 $\beta$ interacts with NMDAR to trigger DSI

Having identified IL-1 $\beta$  and NMDA as two signaling molecules that trigger DSI, we next examine if they interact to trigger DSI. Before the discovery of DSI as a novel neurotoxic pathway (Joshi et al., 2019), substantial evidence has already established that a synergistic, reciprocal functional interaction exists between IL-1 $\beta$  and NMDAR to induce excitotoxicity (Viviani et al., 2003). Because both IL-1 $\beta$  and NMDARs are implicated in excitotoxicity in multiple sclerosis (MS), studying how IL-1 $\beta$  and NMDAR interact to trigger the novel DSI pathway will lead to new insight on pathology of MS. Does the known IL-1 $\beta$ /NMDAR interaction converge onto DSI?

#### Blocking NMDAR versus SNPH-KO gives similar protection to IL-1 $\beta$ toxicity

To examine if NMDA interacts with IL-1 $\beta$ /DSI toxicity, we measured protection of IL-1 $\beta$  toxicity by blocking NMDAR with MK801, then compared this protection with that obtained by blocking SNPH via SNPH-KO. Figure 8 shows that MK801 ( $10 \mu\text{M}$ ) protects against neuronal loss after a 24 h IL-1 $\beta$  stress. Interestingly, this protection by MK801 is similar to that produced by SNPH-KO. Further, combining MK801 and SNPH-KO yields a protection similar to that produced by either one alone. This hints at, but does not prove, that IL-1 $\beta$  and NMDAR might use a common pathway involving SNPH in generating toxicity.

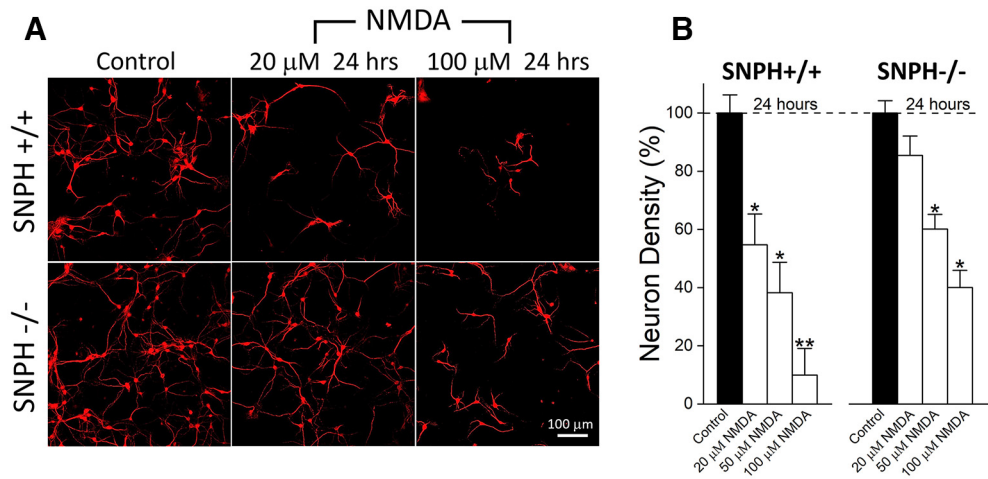


**Figure 7.** NMDA neurotoxicity protection by SNPH-KO. Neurotoxicity assays for NMDA were conducted similar to those for IL-1 $\beta$  in Figure 4. Briefly, cultures were plated at equal density and stained with MAP2, and neuronal death during NMDA stress was assayed by counting MAP2-positive neuronal soma density. **A**, Representative images of cultured hippocampal SNPH<sup>+/+</sup> and SNPH<sup>-/-</sup> neurons in control without NMDA and after 24 h NMDA stress (20  $\mu$ M, 100  $\mu$ M). **B**, Quantitative analysis of MAP2-positive neuron soma density in SNPH<sup>+/+</sup> and SNPH<sup>-/-</sup> neurons after 24 h treatment with 20  $\mu$ M, 50  $\mu$ M, and 100  $\mu$ M NMDA. There is complete protection of NMDA-induced neuronal loss by SNPH<sup>-/-</sup> at 20  $\mu$ M and strong, although incomplete, protection by SNPH<sup>-/-</sup> at 50  $\mu$ M and 100  $\mu$ M NMDA.  $N = 3$  coverslips/group of SNPH<sup>+/+</sup> and SNPH<sup>-/-</sup> with 30 images analyzed per group.

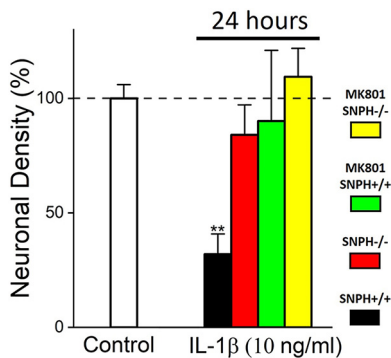


**Figure 8.** Blocking NMDAR gives similar protection to IL-1 $\beta$  toxicity as SNPH-KO. Neuronal density (MAP2-positive soma) measured at 24 h under IL-1 $\beta$  (10 ng/ml) stress for SNPH<sup>+/+</sup>, SNPH<sup>-/-</sup>, SNPH<sup>+/+</sup> plus MK-801, and SNPH<sup>-/-</sup> plus MK-801 (10  $\mu$ M,  $N = 3$ , \*\* $p < 0.01$ ). MK-801 is a generic blocker for NMDAR. The controls are SNPH<sup>+/+</sup>, SNPH<sup>-/-</sup>, SNPH<sup>+/+</sup> plus MK-801, and SNPH<sup>-/-</sup> plus MK-801, respectively, without IL-1 $\beta$  for each group but merged into a single control at 100% for all groups.

**Blocking NMDAR prevents IL-1 $\beta$  from triggering DSI**

To further explore possible interactions between IL-1 $\beta$  and NMDAR, we next asked how blocking NMDAR might ameliorate IL-1 $\beta$  toxicity. As our guiding hypothesis is that the DSI triggered by IL-1 $\beta$  underlies IL-1 $\beta$  toxicity, we therefore examined if blocking NMDAR ameliorated IL-1 $\beta$  toxicity by preventing IL-1 $\beta$  from triggering DSI. Figure 9E shows DSI triggered by a 24 h IL-1 $\beta$  stress over control (Fig. 9D) under high-magnification orthogonal analysis. Intriguingly, blocking NMDAR with MK801 prevents IL-1 $\beta$  from triggering DSI (Fig. 9F), as quantified by the bar chart on the right (Fig. 9G). As we have already demonstrated that NMDA itself triggers DSI (Fig. 6N), the results of Figure 9 that blocking NMDAR blocks IL-1 $\beta$  from triggering DSI suggest that IL-1 $\beta$  uses NMDAR as an intermediary to trigger DSI.

**Functional coupling between IL-1 $\beta$  and NMDAR is required for DSI induction**

To further examine possible interactions between IL-1 $\beta$  and NMDAR in triggering DSI, we relied on a study by Viviani et al.

(2003), who demonstrated that IL-1 $\beta$  interacts with NMDAR via tyrosine kinases. Viviani et al. (2003) showed that the IL-1 $\beta$ /NMDAR interaction can be decoupled by tyrosine kinase inhibitors Lavendustin A (500 nM) and PP2 (1  $\mu$ M). We therefore asked if decoupling the IL-1 $\beta$ /NMDAR interaction by these two tyrosine kinase inhibitors prevents either IL-1 $\beta$  or NMDA from triggering DSI.

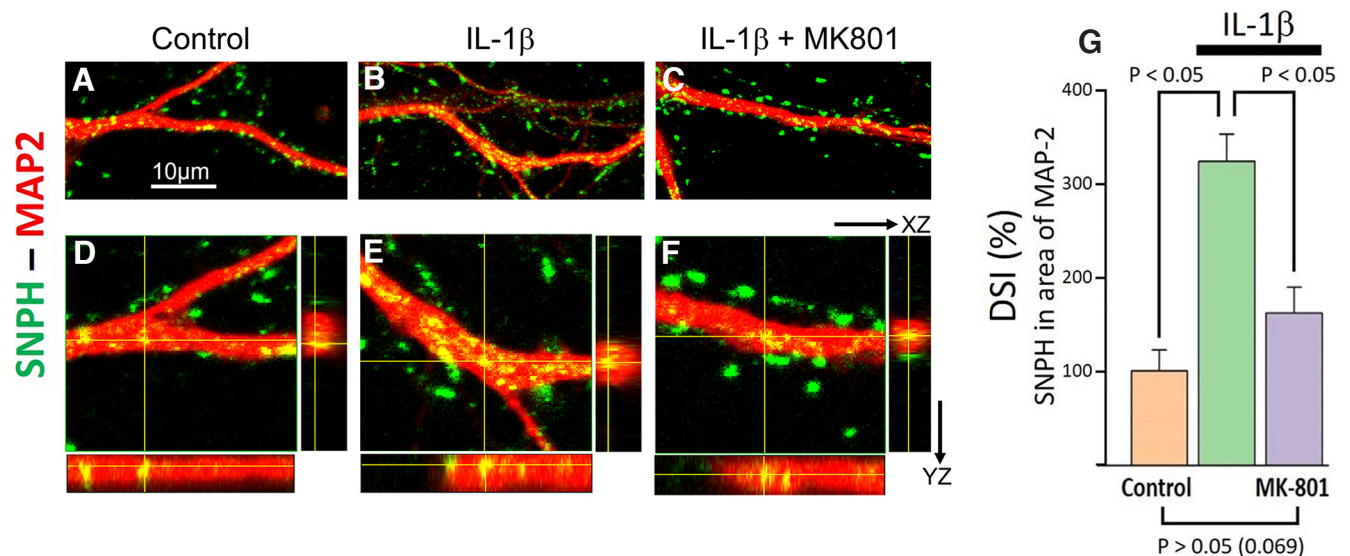
**Lavendustin prevents IL-1 $\beta$  from triggering DSI**

Figure 10, A–C, shows the effect of Lavendustin A (500 nM) on DSI induced by IL-1 $\beta$  using orthogonal analysis. Dendrites from cultured neurons were double stained with SNPH and dendritic marker MAP2. In control dendrites little or no DSI was observed (Fig. 10A). A 24 h stress with IL-1 $\beta$  causes a massive increase in SNPH inside dendrites (Fig. 10B) verified by orthogonal analysis of the merged image (Fig. 10B). Intriguingly, this IL-1 $\beta$ -triggered DSI was blocked by Lavendustin (Fig. 10C), which according to Viviani et al. (2003), decouples the interaction between IL-1 $\beta$  and NMDAR. Quantification analysis of the inhibitory effects on DSI by Lavendustin, as well as by the other tyrosine kinase inhibitor PP2 from Viviani et al. (2003), is shown in Figure 10D. Interestingly, Lavendustin is more powerful than PP2 in inhibiting the IL-1 $\beta$ -triggered DSI at the concentrations used by Viviani et al. (2003). It is possible that Lavendustin blocks IL-1 $\beta$  from triggering DSI independent of NMDAR. Nevertheless, given that Viviani et al. (2003) have already demonstrated that Lavendustin decouples the reciprocal interaction between IL-1 $\beta$  and NMDAR, it is reasonable to suggest that intact coupling between IL-1 $\beta$  and NMDAR is required for DSI induction. We therefore hypothesize that the interaction between IL-1 $\beta$  and NMDAR described by Viviani et al. (2003) is an upstream signal that converges downstream to a new locus, the DSI. Finally, we confirmed that the IL-1R antagonist IL-1ra blocks IL-1 $\beta$  from triggering DSI (Fig. 10D).

**Lavendustin prevents NMDA from triggering DSI**

In addition to preventing IL-1 $\beta$  from triggering DSI, we also examined if Lavendustin similarly prevents NMDA from triggering DSI. Figure 11 shows the effect of Lavendustin A (500 nM) on DSI induced by NMDA. Dendrites were double stained with





**Figure 9.** Blocking NMDAR blocks IL-1 $\beta$  from triggering DSI. Orthogonal analysis shows that blocking NMDAR with MK801 blocks IL-1 $\beta$  from triggering DSI. *A–C*, Triplicate of cultured neuron dishes in each group, (*A*) Control, (*B*) IL-1 $\beta$  (10 ng/ml), and (*C*) IL-1 $\beta$  + MK801 (10  $\mu$ M). *D–F*, Bottom, Corresponding orthogonal analysis for DSI at high magnification. MK801 (10  $\mu$ M) was applied 5 min before adding IL-1 $\beta$ . Green is SNPH, and red is MAP2 stained dendrites. *G*, Quantitative analysis of DSI triggered by IL-1 $\beta$  and blocked by MK-801. Ten 3-D volume scan (z-series scan) images were collected, and dendrites of 10 neurons were analyzed from each dish with orthogonal analysis with NIS-Elements and ImageJ software.

MAP2 and SNPH. A 24 h stress with NMDA causes a significant increase in SNPH inside dendrites (Fig. 11*B*) over control (Fig. 11*A*) verified by orthogonal analysis of the merged image (Fig. 11*B*). Also shown in Figure 11 are the individual MAP2 images (middle) and SNPH images (bottom). Importantly, as in the case of IL-1 $\beta$  (Fig. 10*A–C*), the DSI triggered by NMDA was also blocked by Lavendustin (Fig. 11*C*), as further quantified in Figure 11*D*.

Collectively, these results suggest that intact coupling between IL-1 $\beta$  and NMDAR is required for DSI induction. First, direct treatment with either IL-1 $\beta$  or NMDA triggers DSI. Second, decoupling the known IL-1 $\beta$ /NMDAR interaction by the tyrosine kinase inhibitor Lavendustin (Viviani et al., 2003) prevents either IL-1 $\beta$  (Fig. 10) or NMDA (Fig. 11) from triggering DSI. We therefore suggest that the known reciprocal interaction between IL-1 $\beta$ /NMDAR (Viviani et al., 2003) converges onto a novel pathologic locus, the DSI (Fig. 12*B,C*).

## Discussion

In a normal nervous system, the mitochondrial anchor SNPH in neurons is selectively expressed in axons with little or no expression in dendrites (Kang et al., 2008). This normal expression of SNPH in axons is important for neuronal health by positioning mitochondria along axons to match metabolic needs. In 2019 we discovered that in certain disease models, there is a misplacement of SNPH into neuronal dendrites. The consequence is a novel form of neurodegeneration,

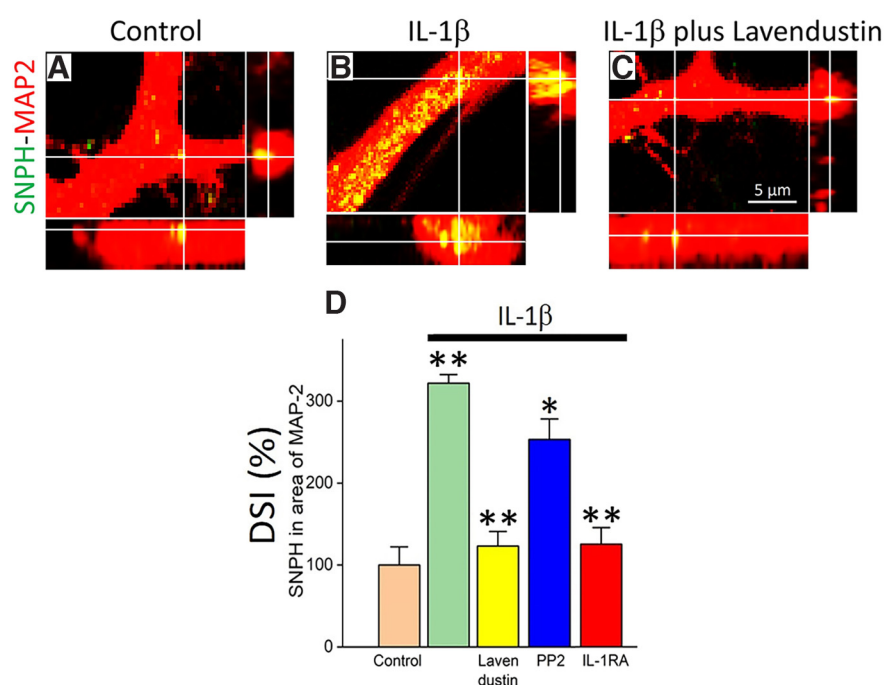


**Figure 10.** Tyrosine kinase inhibitor prevents IL-1 $\beta$  from triggering DSI. *A–C*, Merged images of SNPH-MAP2 staining of cultured hippocampal neurons showing IL-1 $\beta$  (10 ng/ml, 24 h) triggered massive DSI (*B*) that is blocked by 30 min pretreatment with Lavendustin (*C*, 500 nM). For DSI, the SNPH puncta are inside dendrites and turn yellow in the merged SNPH-MAP2 images (top) as verified by orthogonal analysis (bottom and right images). *D*, Quantification of the inhibitory effects of tyrosine kinase inhibitors Lavendustin (500 nM) and PP2 (1  $\mu$ M) on DSI induced by IL-1 $\beta$ . Also shown for comparison are inhibitory effects of IL-1r antagonist IL-1RA (0.5  $\mu$ g/ml) on DSI induced by IL-1 $\beta$ . All agents were applied 30 min before application of IL-1 $\beta$  (10 ng/ml).  $N = 30$  dendrites for each group ( $**p < 0.005$  between Control and IL-1 $\beta$ , between IL-1 $\beta$  and Lavendustin, between IL-1 $\beta$  and IL-1RA;  $*p < 0.05$  between IL-1 $\beta$  and PP2). No significant differences are found among Control, Lavendustin, and IL-1RA.

termed DSI, in which dendrites become sensitized to excitotoxicity (Joshi et al., 2019). A major unanswered issue since the work of Joshi et al. (2019) concerns the pathologic signals that trigger misplacement of SNPH into dendrites. In this article we identified two key players in excitotoxicity that not only

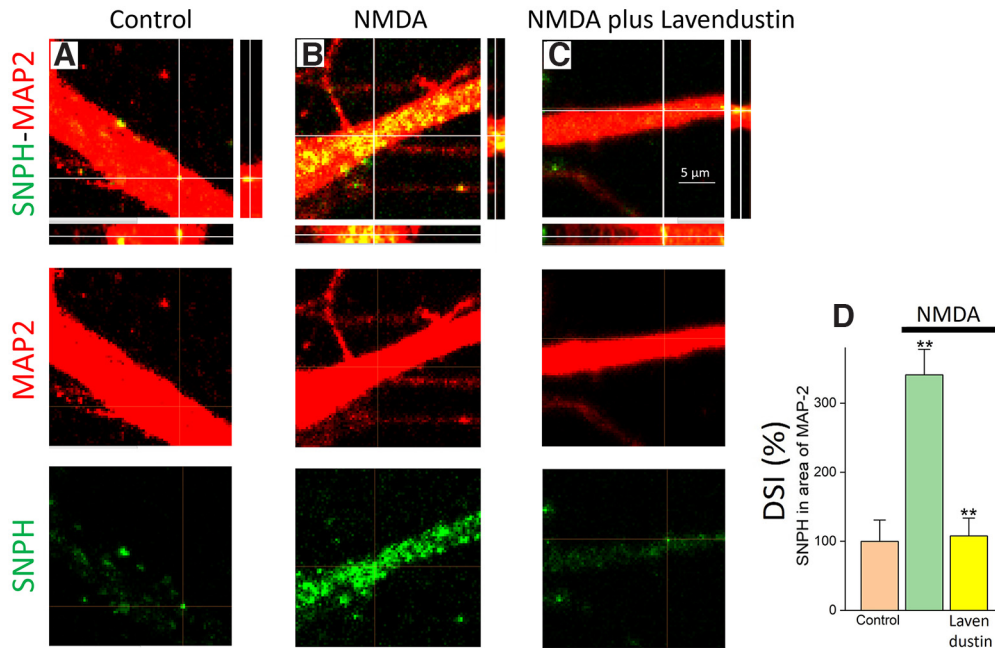


**Figure 11.** Tyrosine kinase inhibitor prevents NMDA from triggering DSI. **A–C**, Merged images of SNPH-MAP2 staining of cultured hippocampal neurons showing NMDA (10  $\mu$ M, 24 h) triggered massive DSI (**B**) that is blocked by 30 min pretreatment with Lavendustin A (**C**, 500 nM). For DSI, the SNPH puncta are inside dendrites and turn yellow in the merged SNPH-MAP2 images (top) as verified by orthogonal analysis (bottom and right images). Middle, MAP2 staining dendrites. Bottom, SNPH staining syntaphilin. **D**, Quantification of the inhibitory effects of tyrosine kinase inhibitor Lavendustin (500 nM) on DSI induced by NMDA.  $N = 30$  dendrites for each group (\*\* $p < 0.005$  between Control and NMDA and \*\* $p < 0.005$  between NMDA and Lavendustin; no significant difference found between Control and Lavendustin).

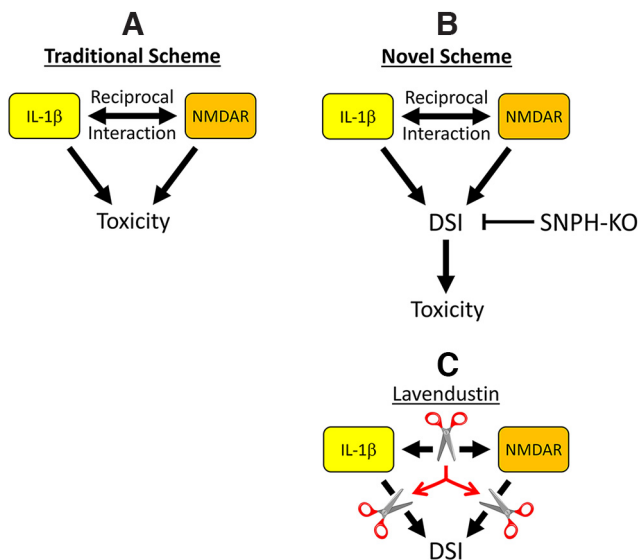


**Figure 12.** Novel tripartite signaling axis among IL-1 $\beta$ , NMDAR, and DSI in neurotoxicity. **A**, Traditional scheme. Viviani et al. (2003) demonstrated that IL-1 $\beta$  undergoes reciprocal interaction with NMDAR via tyrosine kinases to trigger excitotoxicity. **B**, Novel scheme. Tripartite signaling axis between IL-1 $\beta$ , NMDAR, and DSI in neuronal toxicity. We hypothesize that the traditional IL-1 $\beta$ /NMDAR interaction converges to a novel excitotoxic locus, the DSI. SNPH-KO ameliorates IL-1 $\beta$ /NMDAR toxicity by blocking DSI, the novel locus identified in this article at which IL-1 $\beta$ /NMDAR converges. **C**, Intact coupling between IL-1 $\beta$  and NMDAR is required for DSI induction. Decoupling the IL-1 $\beta$ /NMDAR interaction by tyrosine inhibitor Lavendustin disables either IL-1 $\beta$  or NMDA from triggering DSI.

trigger DSI but does so in an interactive fashion, the inflammatory cytokine IL-1 $\beta$  and NMDAR.

Our novel hypothesis is summarized in Figure 12. In the traditional scheme (Fig. 12A), IL-1 $\beta$  and NMDAR interact synergistically to cause neuronal toxicity (Viviani et al., 2003). In

our novel scheme (Fig. 12B), this IL-1 $\beta$ /NMDAR interaction converges to a new locus, the DSI, to cause neuronal toxicity. We further suggest that intact coupling between IL-1 $\beta$  and NMDAR is required for DSI induction (Fig. 12C). Specifically, decoupling the interaction between IL-1 $\beta$  and NMDAR via the tyrosine kinase inhibitor Lavendustin (Viviani et al., 2003) disables this IL-1 $\beta$ /NMDAR/SNPH signaling axis, preventing DSI induction by either NMDA or IL-1 $\beta$  (Fig. 12C). Finally, SNPH-KO ameliorates both IL-1 $\beta$  (Fig. 4) and NMDA (Fig. 7) toxicity, presumably by blocking DSI, the locus at which IL-1 $\beta$  and NMDAR converge.

We discuss three aspects of our finding. First, does IL-1 $\beta$  and NMDAR interact synergistically in triggering DSI to amplify inflammatory damage? Second, is self-induction of DSI by NMDA a novel mechanism in NMDA excitotoxicity? Third, is DSI a new strategic site for therapeutic intervention in inflammatory MS.

**Interaction between IL-1 $\beta$  and NMDAR in triggering DSI: additive or synergistic?**

Although we have demonstrated that IL-1 $\beta$  and NMDAR are not independent but interact with each other in triggering DSI, outstanding questions remain regarding the nature of this interaction. A key question is whether IL-1 $\beta$  and NMDAR interact additively or synergistically to trigger DSI. If IL-1 $\beta$  undergoes reciprocal interaction with NMDAR (Viviani et al., 2003) before converging to DSI, would subthreshold preconditioning either NMDAR or the IL-1 $\beta$  receptor (IL-1R) greatly sensitize subsequent DSI induction? For example, Viviani et al. (2003) demonstrated that preconditioning cultured neurons with low dosage IL-1 $\beta$ , although producing no toxic effects per se, significantly increased subsequent NMDA-induced neuronal death. Would similar low dosage IL-1 $\beta$  preconditioning significantly amplify subsequent induction of DSI by NMDA? Reciprocally, would

preconditioning NMDAR also amplify subsequent induction of DSI by IL-1 $\beta$ ? Finally, would NMDAR or IL-1R preconditioning, even though each alone has no effect on DSI, synergistically induce robust toxic DSI when combined? These important questions will be best addressed in complex systems with intact neuron-glia connectivity. For example, NMDA may induce the release of cofactors in an intact neural circuitry to affect the status of IL-1R, and the status of IL-1R could reciprocally amplify NMDAR to induce more DSI. Likewise, IL-1 $\beta$  could induce glutamate release from neurons through action on glutaminase (Ye et al., 2013) or the release of other factors from neighboring cells to amplify the interaction between IL-1 $\beta$  and NMDAR to induce stronger DSI. Synergistic interaction between excitotoxicity players IL-1 $\beta$  and NMDA in inducing DSI would greatly amplify damage done by each alone. If true, targeting DSI would be a sensitive and strategic locus to block this synergistic interaction to turn off excitotoxicity.

### Is self-induction of DSI by NMDA a novel mechanism in NMDA excitotoxicity?

NMDA excitotoxicity is a well-established phenomenon. There is an acute phase where damage is related to excessive calcium influx via the NMDAR ionophore. However, there is a secondary slower phase of damage that is linked to complex interplay of various cell death pathways. For example, it has been postulated that there is a toxic coupling between extrasynaptic NMDAR and mitochondria located at the dendritic shaft (Bading, 2017). Here, we propose that a novel mechanism to exacerbate long-term NMDA excitotoxicity is self-induction of DSI by NMDA. Specifically, we hypothesize that during long-term NMDA stress, NMDA concomitantly induces DSI, which amplifies the toxic linkage between extrasynaptic NMDAR and mitochondria. First, we have already demonstrated that DSI occurs selectively at the dendritic shaft (Joshi et al., 2019). Second, a brief 30 min NMDA exposure to 10  $\mu$ M NMDA does not kill neurons but will do so if DSI was artificially induced by prior plasmid transfection (Joshi et al., 2019). This suggests that if NMDA exposure is prolonged, the self-induction of DSI by NMDA will kill neurons. We confirmed this by showing that prolonged treatment of NMDA did kill neurons, but this toxicity can be protected by SNPH-KO (Fig. 7). Hence, we suggest that self-induction of DSI by NMDA is a novel mechanism for NMDA excitotoxicity in prolonged NMDA exposure, and targeting DSI by SNPH-KO is a new therapeutic approach to treat excitotoxicity.

### Implications for multiple sclerosis: is DSI a strategic site for therapeutic intervention?

The toxic DSI pathway was first discovered in the gray matter of a noninflammatory model for progressive MS (Joshi et al., 2019). However, the majority of MS (>90%) is an inflammatory disease. The demonstration in this work that a key inflammatory molecule, the pro-inflammatory cytokine IL-1 $\beta$ , triggers DSI means that this toxic DSI pathway could be relevant to all classes of MS. How might DSI that affects predominantly gray matter be relevant to MS? Although MS has been classically regarded as a demyelinating pathology of the white matter, it has become increasingly clear that gray matter pathology (dendrites/synapse dysfunction) is an independent event in MS triggered by glutamate excitotoxicity and cytokine exposure (Centonze et al., 2010; Klaver et al., 2013; Mandolesi et al., 2013; Rossi et al., 2014; Calabrese et al., 2015).

The cytokine IL-1 $\beta$  plays important pathologic roles in inflammatory models of MS and human MS (Burm et al., 2016; Lin and Edelson, 2017; Paré et al., 2017, 2018). A common consequence of IL-1 $\beta$  action in gray matter is dendritic/synaptic pathology. For example, cognitive deficits linked to gray matter damage has long been known to be a common symptom of MS (Rao et al., 1991). In a previous study, Hou et al. (2020) demonstrated that activation of the NLRP3 inflammasome, a key pathway for releasing IL-1 $\beta$ , is linked to memory deficits and dendritic fragmentation in the hippocampus of experimental autoimmune encephalomyelitis (EAE), a rodent model for inflammatory MS. Further, inhibition of IL-1 $\beta$  release by blocking NLRP3 inflammasomes dramatically prevents dendritic fragmentation and restores memory deficits (Hou et al., 2020). Strikingly, the dendritic fragmentation observed by Hou et al. (2020) in the EAE hippocampus is very similar to the dendritic fragmentation in cultured hippocampal neurons exposed to IL-1 $\beta$  in our study (Fig. 4, right). Further, this dendritic damage is prevented either by blocking IL-1 $\beta$  release by inhibiting NLRP3 inflammasomes in EAE *in vivo* (Hou et al., 2020) or by SNPH-KO in the presence of IL-1 $\beta$  *in vitro* (Fig. 4, right). Collectively, we hypothesize that induction of toxic DSI by IL-1 $\beta$  is the common locus for dendritic damage underlying hippocampal dysfunction and memory deficits in the inflammatory EAE model for MS. It is important to emphasize that our study only addresses one particular cytokine, the IL-1 $\beta$ . The intriguing possibility remains that other pro-inflammatory cytokine members could also trigger DSI as a common downstream pathway to damage gray matter. If true, targeting DSI could be an exciting common strategic therapy to prevent diverse inflammatory insults in MS.

Finally, although DSI was first discovered in MS models (Joshi et al., 2019), our finding that DSI is triggered by pro-inflammatory cytokines suggests that pathologic signaling because of misplacement of SNPH in neuronal dendrites could be relevant to other neurologic or psychological diseases with inflammation. For example, neuroinflammation is a hallmark of many neurodegenerative diseases, including innate immune system activation, microglia activation, and cytokine production in Alzheimer's disease (Lee et al., 2021); T cell activation and cytokine activation in Parkinson's disease (Williams et al., 2021); and T cell activation in amyotrophic lateral sclerosis (Rolfes et al., 2021). Whether DSI occurs in these diseases is completely unexplored. It is well established that SNPH is a key microtubule-based regulator of axonal mitochondrial trafficking and anchoring in mature neurons that is highly relevant to CNS diseases (Cheng and Sheng, 2021). According to our current finding, any inflammation component in neurodegenerative diseases could exacerbate the toxic role of SNPH by causing misplacement of SNPH into dendrites to cause novel pathology described in this article.

### References

- Bading H (2017) Therapeutic targeting of the pathological triad of extrasynaptic NMDA receptor signaling in neurodegenerations. *J Exp Med* 214:569–578.
- Burm SM, Peferoen LAN, Zuiderwijk-Sick EA, Haanstra KG, 't Hart BA, van der Valk P, Amor S, Bauer J, Bajramovic JJ (2016) Expression of IL-1 $\beta$  in rhesus EAE and MS lesions is mainly induced in the CNS itself. *J Neuroinflammation* 13:138.
- Calabrese M, Magliozzi R, Ciccarelli O, Geurts JGG, Reynolds R, Martin R (2015) Exploring the origins of grey matter damage in multiple sclerosis. *Nat Rev Neurosci* 16:147–158.



- Centonze D, Muzio L, Rossi S, Furlan R, Bernardi G, Martino G (2010) The link between inflammation, synaptic transmission and neurodegeneration in multiple sclerosis. *Cell Death Differ* 17:1083–1091.
- Cheng XT, Sheng ZH (2021) Developmental regulation of microtubule-based trafficking and anchoring of axonal mitochondria in health and diseases. *Dev Neurobiol* 81:284–299.
- Chiu DN, Jahr CE (2017) Extracellular glutamate in the nucleus accumbens is nanomolar in both synaptic and non-synaptic compartments. *Cell Rep* 18:2576–2583.
- Danbolt NC (2001) Glutamate uptake. *Prog Neurobiol* 65:1–105.
- Herman MA, Jahr CE (2007) Extracellular glutamate concentration in hippocampal slice. *J Neurosci* 27:9736–9741.
- Hou B, Zhang Y, Liang P, He Y, Peng B, Liu W, Han S, Yin J, He X (2020) Inhibition of the NLRP3-inflammasome prevents cognitive deficits in experimental autoimmune encephalomyelitis mice via the alteration of astrocyte phenotype. *Cell Death Dis* 11:377.
- Jabaudon D, Shimamoto K, Yasuda-Kamatani Y, Scanziani M, Gähwiler BH, Gerber U (1999) Inhibition of uptake unmasks rapid extracellular turnover of glutamate of nonvesicular origin. *Proc Natl Acad Sci U S A* 96:8733–8738.
- Jiajia L, Shinghung M, Jiacheng Z, Jialing W, Dilin X, Shengquan H, Zaijun Z, Qinwen W, Yifan H, Wei C (2017) Assessment of neuronal viability using fluorescein diacetate-propidium iodide double staining in cerebellar granule neuron culture. *J Vis Exp* 2017:55442.
- Joshi DC, Singh M, Krishnamurthy K, Joshi PG, Joshi NB (2011) AMPA induced Ca<sup>2+</sup> influx in motor neurons occurs through voltage gated Ca<sup>2+</sup> channel and Ca<sup>2+</sup> permeable AMPA receptor. *Neurochem Int* 59:913–921.
- Joshi DC, Zhang C-L, Babujee L, Vevea JD, August BK, Sheng Z-H, Chapman ER, Gomez TM, Chiu SY (2019) Inappropriate intrusion of an axonal mitochondrial anchor into dendrites causes neurodegeneration. *Cell Rep* 29:685–696.e5.
- Kang J-S, Tian J-H, Pan P-Y, Zald P, Li C, Deng C, Sheng Z-H (2008) Docking of axonal mitochondria by syntaphilin controls their mobility and affects short-term facilitation. *Cell* 132:137–148.
- Klaver R, de Vries HE, Schenk GJ, Geurts JGG (2013) Grey matter damage in multiple sclerosis: a pathology perspective. *Prion* 7:66–75.
- Lee S, Cho HJ, Ryu JH (2021) Innate immunity and cell death in Alzheimer's disease. *ASN Neuro* 13:17590914211051908.
- Lin C-C, Edelson BT (2017) New insights into the role of IL-1 $\beta$  in experimental autoimmune encephalomyelitis and multiple sclerosis. *J Immunol* 198:4553–4560.
- Mandolesi G, Musella A, Gentile A, Grasselli G, Haji N, Sepman H, Fresegna D, Bullitta S, de Vito F, Musumeci G, di Sanza C, Strata P, Centonze D (2013) Interleukin-1 $\beta$  alters glutamate transmission at Purkinje cell synapses in a mouse model of multiple sclerosis. *J Neurosci* 33:12105–12121.
- Paré A, Mailhot B, Lévesque SA, Lacroix S (2017) Involvement of the IL-1 system in experimental autoimmune encephalomyelitis and multiple sclerosis: breaking the vicious cycle between IL-1 $\beta$  and GM-CSF. *Brain Behav Immun* 62:1–8.
- Paré A, Mailhot B, Lévesque SA, Juzwik C, Ignatius Arokia Doss PM, Lécuyer M-A, Prat A, Rangachari M, Fournier A, Lacroix S (2018) IL-1 $\beta$  enables CNS access to CCR2(hi) monocytes and the generation of pathogenic cells through GM-CSF released by CNS endothelial cells. *Proc Natl Acad Sci U S A* 115:E1194–E1203.
- Rakotomamonjy J, Gumez-Gamboa A (2019) Purkinje cell survival in organotypic cerebellar slice cultures. *JoVE* 2019:e60353.
- Rao SM, Leo GJ, Bernardin L, Unverzagt F (1991) Cognitive dysfunction in multiple sclerosis. *Neurology* 41:685–691.
- Rolfes L, Schulte-Mecklenbeck A, Schreiber S, Vielhaber S, Herty M, Marten A, Pfeuffer S, Ruck T, Wiendl H, Gross CC, Meuth SG, Boentert M, Pawlitzki M (2021) Amyotrophic lateral sclerosis patients show increased peripheral and intrathecal T-cell activation. *Brain Commun* 3:fcab157.
- Rossi S, Motta C, Studer V, Macchiarulo G, Volpe E, Barbieri F, Ruocco G, Buttari F, Finardi A, Mancino R, Weiss S, Battistini L, Martino G, Furlan R, Drulovic J, Centonze D (2014) Interleukin-1 $\beta$  causes excitotoxic neurodegeneration and multiple sclerosis disease progression by activating the apoptotic protein p53. *Mol Neurodegener* 9:56.
- Viviani B, Bartesaghi S, Gardoni F, Vezzani A, Behrens MM, Bartfai T, Binaglia M, Corsini E, di Luca M, Galli CL, Marinovich M (2003) Interleukin-1 $\beta$  enhances NMDA receptor-mediated intracellular calcium increase through activation of the Src family of kinases. *J Neurosci* 23:8692–8700.
- Wang X, Schwarz TL (2009) The mechanism of Ca<sup>2+</sup>-dependent regulation of kinesin-mediated mitochondrial motility. *Cell* 136:163–174.
- Williams GP, Schonhoff AM, Jurkuvenaite A, Gallups NJ, Standaert DG, Harms AS (2021) CD4 T cells mediate brain inflammation and neurodegeneration in a mouse model of Parkinson's disease. *Brain* 144:2047–2059.
- Ye L, Huang Y, Zhao L, Li Y, Sun L, Zhou Y, Qian G, Zheng JC (2013) IL-1 $\beta$  and TNF- $\alpha$  induce neurotoxicity through glutamate production: a potential role for neuronal glutaminase. *J Neurochem* 125:897–908.
- Ying HS, Gottron FJ, Choi DW (2001) Assessment of cell viability in primary neuronal cultures. *Curr Protoc Neurosci* Chapter 7:Unit7.18.